

Diode effect in Fraunhofer patterns of disordered multi-terminal Josephson junctions

Luca Chiroli,^{1,*} Angelo Greco,² Alessandro Crippa,² Elia Strambini,² Mario Cuoco,² Luigi Amico,^{1,3,4} and Francesco Giazotto²

¹*Quantum Research Center, Technology Innovation Institute, Abu Dhabi, UAE*

²*NEST, Istituto Nanoscienze-CNR and Scuola Normale Superiore, I-56127 Pisa, Italy*

³*Dipartimento di Fisica e Astronomia 'Ettore Majorana', Via S. Sofia 64, 95123 Catania, Italy*

⁴*INFN-Sezione di Catania, Via S. Sofia 64, 95127 Catania, Italy*

We study the role of different spatial inhomogeneities in generating the conditions for the appearance of a superconducting diode effect in the Fraunhofer pattern of wide Josephson junctions. Through the scattering matrix approach, we highlight the role of mirror symmetry of the junction in forbidding the diode effect in both the two-terminal and the multi-terminal case. As sources of mirror symmetry breaking, we study spatial potentials of long and short wavelength with respect to the size of the system, mimicking the effect of side gates and atomic scale disorder, respectively, as well as the geometry of the junction, and assess their impact on the diode effect. As a common trend, we observe qualitatively similar rectification patterns magnified at the nodal points of the Fraunhofer pattern by destructing interference. In multi-terminal mirror-symmetric setups, we single out the phase at additional terminals as a controllable knob to tune the diode effect at the finite field. The work presents a comprehensive treatment of the role of pure spatial inhomogeneity in the emergence of a diode effect in wide junctions.

I. INTRODUCTION

Nonreciprocal effects in superconductors manifest as the magnitude of the critical current acquiring a dependence on the direction of the applied current. Such a feature results in the so-called superconducting diode effect (SDE), which aims to rectify the supercurrent in the system. Motivated both by fundamental questions on the underlying generating mechanisms and by the potential technological applications in dissipationless nanoelectronics [1], a large amount of scientific work has recently focused on the SDE [2–7]. It is widely accepted that crucial conditions for the emergence of an SDE are time-reversal and spatial-inversion symmetry breaking, together with high transparency in Josephson junction realizations. Nonreciprocal supercurrents have been measured in quantum materials such as noncentrosymmetric systems [2, 8, 9], where the presence of a Rashba spin-orbit interaction, together with the application of an in-plane magnetic field, yields a simultaneous breaking of spatial-inversion and time-reversal symmetry, resulting in a reciprocity symmetry breaking and a diode effect. Nonreciprocal supercurrents have also been observed in polar two-dimensional superconductors in the superconducting fluctuation state [10], by explicitly breaking spatial inversion symmetry in nanopatterned devices [11], in zero magnetic fields in noncentrosymmetric superconductor/ferromagnet multilayers [12] and in twisted trilayer graphene [13], thus pointing to a time-reversal symmetry breaking state. A diode effect has been proposed and measured for finite-momentum Cooper pairs [13–15], and it has been measured in twisted high T_c superconductors junctions [16, 17].

Focusing on Josephson devices employing conventional superconductors, the SDE has been proposed [18, 19], and measured in Dayem bridges [20] and in interferometric setups involving superconducting quantum interference devices (SQUIDs) [21, 22], owing to a high-harmonic content of the junctions current-phase relation (CPR). It has also been observed in multi-terminal devices [23, 24] and gate-tunable junctions [23, 25], through the back-action-based mechanism [26, 27], through screening currents [28, 29] and self-field effects induced by supercurrents [30, 31], and phase re-configuration induced by the Josephson current and kinetic inductance [32]. It has been proposed to arise in systems hosting helical phases [33–35], multi-band superconductors [36], due to vortex phase textures [37], and through magnetization gradients [38].

In this work, we investigate the Fraunhofer diffraction pattern in wide Josephson junctions and study the role of spatial inhomogeneity in the emergence of a diode effect at finite flux. In a wide Josephson junction, schematically shown in Fig. 1(a), two superconducting terminals are coupled via a central normal region that acts as a diffraction center for the Cooper pairs under a perpendicular magnetic field. The latter acquire a spatially dependent phase that results in the typical interferometric pattern in the critical current. It becomes clear that a spatial inhomogeneity that breaks reciprocity results in a diode effect. We formalize this concept by studying the role of mirror symmetry in the junction through a scattering matrix approach that allows us to make general statements independent of the particular mirror symmetry-breaking realization. We then analyze the Fraunhofer pattern of specific configurations and show that, as a common trend, the SDE is magnified at the nodal points of the interferometric pattern, where destructive interference strongly suppresses the current.

The present study demonstrates that a SDE can

* luca.chiroli@tii.ae

emerge in seemingly different systems characterized by spatial inhomogeneity of different kind and origin. The meeting criteria results to be time-reversal and spatial-inversion symmetry-breaking, together with high junction transparency, as it has been widely experimentally observed.

A. Summary of Results

As the simplest example of a Josephson Fraunhofer interferometer, we first study a circuit of several Josephson junctions connected in parallel. We show that the diode effect appears for highly transparent junctions when a mirror asymmetric spatial inhomogeneity is introduced either in the transmission coefficients or in the phases through a multi-loop structure. This phenomenology has been exploited to optimize the diode effect by suitably engineering the disorder [18, 19], albeit spoiling the Fraunhofer pattern.

We then study wide Josephson junctions and simulate several devices characterized by different kinds of spatial inhomogeneity. Interestingly, we show that a smooth spatially-dependent modulation of the local scalar potential in the central region, resulting from the application of back gates in a two-dimensional semiconducting normal region, can result in the appearance of an SDE. However, apart from the central lobe of the Fraunhofer pattern, the rectification efficiency does not seem to be correlated with the value of the gate potential. Analogously, a short wavelength disorder or a non-mirror-symmetric geomet-

rical shape of the central area also produces an SDE in the interference pattern in a qualitatively similar way. A maximum rectification is always observed around the nodes of the interference pattern. At that point, one of the two critical currents, either the positive or the negative, can experience a substantial suppression due to destructive interference. As overall effect, the SDE results to be amplified.

As an interesting variation to the two-terminal junction, we also consider a multi-terminal junction, with a main wide two-terminal junction structure and additional lateral superconducting terminals that introduce their phase as a knob to modulate the Fraunhofer pattern. We indeed see that such a configuration can allow for the tuning of the diode effect at finite magnetic flux, thus extending the results on multi-terminal SDE [23, 24] to the case of the Fraunhofer interference pattern.

The work is structured as follows. In Sec. II, we present the general theoretical framework based on the scattering matrix approach to calculate the Josephson currents in multi-terminal Fraunhofer systems, and we study the conditions of mirror symmetry breaking for the appearance of the diode effect. In Sec. III, we study a multi-loop parallel of highly transmissive Josephson junctions as the most straightforward system to show a Fraunhofer interference pattern in the critical current and investigate the role of transmission and phase disorder. In Sec. IV, we present the results for a wide junction with several kinds of mirror symmetry breaking, from local long wavelength and short wavelength potential modulations to spatial mirror symmetry breaking in the system geometry. In Sec. V, we extend the analysis to multi-terminal Josephson devices, and in Sec. VI, we summarize the work results.

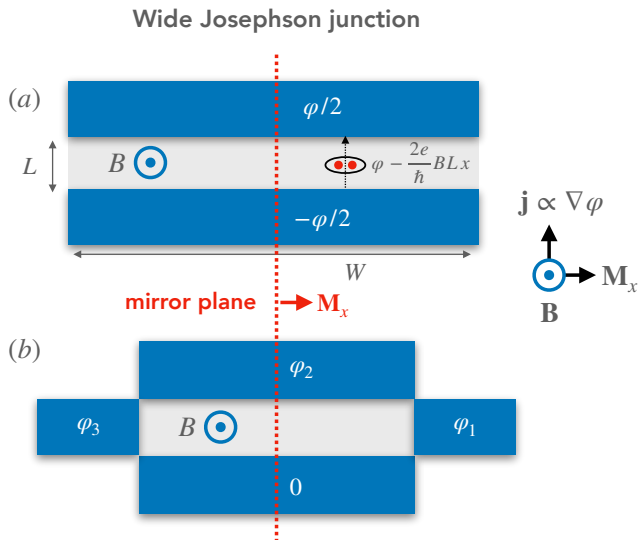


FIG. 1. Schematics of a wide Josephson junction, where a magnetic field yields a position-dependent phase that induces a diffractive Fraunhofer pattern in the critical current. The mirror symmetry plane is determined by the cross-product between the current and the magnetic field. (a) two-terminal case and (b) four-terminal case.

II. SCATTERING MATRIX FORMULATION

We start by setting the framework for studying the diode effect in general Josephson junction systems. The Josephson current through the junction can be described using the scattering matrix formalism [39–41], where the normal central region acts as a scattering region that connects external superconducting leads. The superconducting gap in the leads induces Andreev reflection, which converts carriers at energy ϵ from particle-like to hole-like character and adds a phase shift $e^{-i\arccos(\epsilon/\Delta)}e^{i\varphi_\alpha}$, with $\Delta e^{i\varphi_\alpha}$ the superconducting gap in the leads α . In a two-terminal device, the CPR is given by the equilibrium current in the system, which can be expressed through the free energy of the system $F(\varphi)$ at temperature T [42],

$$I(\varphi) = \frac{2\pi}{\Phi_0} \frac{\partial F(\varphi)}{\partial \varphi}, \quad (1)$$

with $\Phi_0 = h/2e$ the superconducting flux quantum. The free energy can be expressed through the subgap Andreev spectrum [39, 40], and the critical currents for positive

and negative bias currents are defined as

$$I_c^+ = \max_{\varphi} I(\varphi), \quad I_c^- = \min_{\varphi} I(\varphi), \quad (2)$$

and the efficiency of the diode effect is quantified by the rectification coefficient

$$\eta = \frac{I_c^+ - |I_c^-|}{I_c^+ + |I_c^-|}. \quad (3)$$

We are interested in the dependence of the critical currents on the external flux Φ_x produced by an orbital magnetic field threading the scattering region. From the Onsager reciprocity relations, it follows that, in general, we have $I_c^+(\Phi_x) = -I_c^-(-\Phi_x)$. In particular, we demonstrate that we have $I_c^+(\Phi_x) = -I_c^-(\Phi_x)$ for a mirror symmetric system.

Knowing the scattering matrix $s(\epsilon)$ describing the central normal region and assuming its dependence on the energy ϵ can be neglected on the scale of the gap Δ , we can obtain the Andreev spectrum by solving the secular equation [41] (see Appendix A)

$$\begin{pmatrix} 0 & A \\ A^\dagger & 0 \end{pmatrix} \psi = \frac{\epsilon}{\Delta} \psi, \quad (4)$$

where the complex symmetric matrix A is given by

$$A = \frac{1}{2}(r_A s + s^T r_A), \quad (5)$$

where $r_A = \text{diag}(e^{-i\varphi/2} \mathbb{1}_L, e^{i\varphi/2} \mathbb{1}_R)$ and $\mathbb{1}_{L(R)}$ are identity matrices with the dimension of the number of open transport channels in the $L(R)$ lead. By construction, the eigenproblem Eq. (4) is particle-hole symmetric, and the singular values of A uniquely determine the spectrum. In the presence of time-reversal symmetry, the scattering matrix is symmetric, $s^T = s$, and for a two-terminal device, it is possible to express the scattering matrix through the polar decomposition [41, 43]. It follows that the Andreev spectrum acquires the general energy-phase relation (EPR) form $E^\pm(\varphi) = \pm \sum_p E_p(\varphi)$, with

$$E_p(\varphi) = -\Delta \sqrt{1 - \tau_p \sin^2(\varphi/2)}, \quad (6)$$

where the sum is extended over the open channels of transmission τ_p . The free energy is then obtained by populating the levels according to a Fermi-Dirac distribution centered at zero energy.

A. Absence of diode effect in the presence of mirror symmetry

The cross-product between the orbital magnetic field and the phase gradient defines the mirror plane relevant to the diode effect, as shown in Fig. 1(a). For a current flowing along the y -direction and a magnetic field along the z -direction, the relevant mirror plane is then the one

orthogonal to the x axis, M_x , such that $M_x x M_x^{-1} = -x$. For a general scattering matrix s that is mirror-symmetric in the absence of the external field, we can write

$$M_x s(\Phi_x) M_x^{-1} = s(-\Phi_x). \quad (7)$$

This results from the fact that we can always choose a gauge for the vector potential $\mathbf{A}(\mathbf{r})$ describing the magnetic field $\mathbf{B} = (0, 0, B)$ along the z direction such that the only non-zero component is $A_y(x) = Bx$. In this case, the orbital magnetic field is the only source of mirror symmetry breaking, which changes signs under mirror transformation.

Furthermore, by the Onsager reciprocity relations we know that $s^T(\Phi_x) = s(-\Phi_x)$, from which it follows that under mirror transformation the matrix A satisfies

$$M_x A(\varphi, \Phi_x) M_x^{-1} = r_A A(-\varphi, \Phi_x) r_A. \quad (8)$$

Since the singular values of A give the Andreev spectrum, it follows that

$$I(\varphi, \Phi_x) = -I(-\varphi, \Phi_x). \quad (9)$$

Without mirror symmetry, a diode effect cannot be ruled out, and its features depend on the system's microscopic or macroscopic spatial details.

B. Multi-terminal case

In a multi-terminal setup composed of N_l leads, we can define $N_l - 1$ independent phase differences φ_α , with $\alpha = 1, \dots, N_l - 1$, with respect to the phase of a reference lead, that is set to zero (see Fig. 1(b)). The associated CPRs are given by the equilibrium currents in the system, which can be expressed utilizing the free energy of the system $F(\varphi)$ at temperature T [42],

$$I_\alpha(\varphi) = \frac{2\pi}{\Phi_0} \frac{\partial F(\varphi)}{\partial \varphi_\alpha}, \quad (10)$$

yielding $N_l - 1$ independent currents, $I_\alpha \equiv I_{0,\alpha}$. The currents between the other terminals can be expressed as $I_{\alpha,\beta} = I_\alpha - I_\beta$. If we apply a bias current between two given terminals and keep the phases on the other terminals fixed, we can define critical currents as

$$I_{c,\alpha}^+ = \max_{\varphi_\alpha} I_\alpha(\varphi), \quad I_{c,\alpha}^- = \min_{\varphi_\alpha} I_\alpha(\varphi), \quad (11)$$

and an associated rectification coefficient

$$\eta_\alpha = \frac{I_{c,\alpha}^+ - |I_{c,\alpha}^-|}{I_{c,\alpha}^+ + |I_{c,\alpha}^-|}. \quad (12)$$

This configuration has been recently realized in Ref. [44], where two of the three-phase differences of a four-terminal junction have been fixed and controlled by external fluxes in a two-loop configuration.

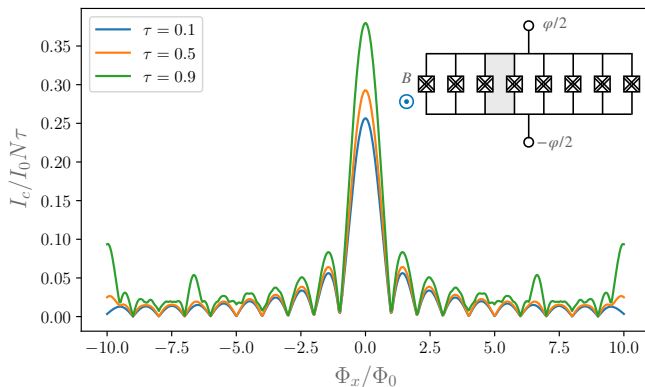


FIG. 2. Interference pattern of the critical current $I_c(\Phi_x)$ of a multi-loop SQUID composed by $N = 20$ junctions as a function of the total flux Φ_x through the junction, as arising from the EPR Eq. (14), for equal junctions of transparency $\tau = 0.1, 0.5, 0.9$. Inset: schematics of a multi-loop SQUID formed by a parallel of several Josephson junctions connected to superconducting leads on the top and the bottom, kept at phase difference φ .

In this work, we are interested in the Fraunhofer interference pattern produced by a magnetic flux threading the area of a wide multi-terminal Josephson junction. The previous formalism can be extended to the multi-terminal case as explained in Ref. [41].

Assuming a geometry of the scattering region and lead arrangements that yield a mirror symmetric multi-terminal scattering matrix s , such that $M_x s(\Phi_x) M_x^{-1} = s(-\Phi_x)$, and under the Onsager reciprocity relations $s^T(\Phi_x) = s(-\Phi_x)$, it follows that

$$I_\alpha(\varphi, \Phi_x) = -I_\alpha(-\varphi_{\mathcal{M}}, \Phi_x), \quad (13)$$

where $\varphi_{\mathcal{M}}$ is a permutation of the phases φ_α that results from the mirror transformation. It then follows that a diode effect appears already at zero field for values of the phases that are not invariant under mirror symmetry. In addition, for values of the phases that are invariant under mirror symmetry, a finite field yields a difference between the positive and negative critical current and a resulting diode effect in the Fraunhofer pattern.

III. MULTIPLE-LOOP SQUID

A parallel of N Josephson junctions, each described by a single harmonic EPR and enclosing $N - 1$ loops threaded by a magnetic flux, was first considered in Ref. [45], where it was shown that a Fraunhofer interference pattern emerges. Furthermore, in Ref. [19], it was first pointed out how a system constituted by a parallel of several highly transparent Josephson junctions can give rise to a very high rectification diode effect. Here, we are interested in the spatial inhomogeneity as a source of the diode effect and the Fraunhofer interference pattern that arises as a function of the applied flux.

A parallel on N high-harmonic-content junctions, each nominally described by an EPR of the form Eq. (6), the total Josephson EPR reads,

$$E(\varphi) = \sum_{j=1}^N E_j(\varphi - 2\pi\Phi_{x,j}/\Phi_0), \quad (14)$$

where $\Phi_{x,j}$ is the total magnetic flux enclosed in the loops before the j -th junction, and we choose the gauge in which the phase φ drops at the first junction. The expression Eq. (14) is a particular case of Eq. (4) that appears when there is no scattering among the different transport channels in a way that the scattering matrix has a block diagonal form in the channels. When expressed in terms of the Fourier components (see Appendix B), the current reads

$$I(\varphi) = -iI_0 \sum_{j=1}^N \sum_{n=1}^{\infty} n \epsilon_{n,j} e^{in(\varphi - \sum_{k<j} \varphi_{x,k})} + \text{c.c.}, \quad (15)$$

where $I_0 = 2\pi\Delta/\Phi_0$ and $\varphi_{x,j} = 2\pi BA_j/\Phi_0$ is the flux through the area A_j of the loop between junctions $j - 1$ and j , in units of $\Phi_0/2\pi$. The expression Eq. (15) meets two fundamental conditions at the same time: *i*) it breaks time-reversal symmetry, and *ii*) it generally breaks mirror symmetry $j \rightarrow N + 1 - j$, thus allowing, in general, the appearance of a diode effect.

For a mirror symmetric system of (single-channel) junctions of equal transparency τ and equal area loops threaded by a total flux $\Phi_x = (N - 1)BA$, with A the area of a single loop, it is easily shown that $I(\varphi, \Phi_x) = I(\varphi + 2\pi(N - 1)\Phi_x/(N\Phi_0), -\Phi_x)$. Recalling the definitions of the critical currents and the Onsager relations, it follows that no diode effect appears for any finite external field. In particular, the current reads

$$I(\varphi) = 2I_0 \sum_{n=1}^{\infty} n \epsilon_n \frac{\sin(\pi n N \Phi_x / (N - 1) \Phi_0)}{\sin(\pi n \Phi_x / (N - 1) \Phi_0)} \times \sin(n(\varphi - \pi \Phi_x / \Phi_0)). \quad (16)$$

The dependence on the external flux of the critical current is shown in Fig. 2, where a Fraunhofer interference pattern appears that is periodic with period $\Phi_x = (N - 1)\Phi_0$, i.e., a flux quantum Φ_0 threading each unit cell (a gray area in the inset of Fig. 2). For low transparency τ the critical current reads

$$I_c(\Phi_x) = \frac{\tau I_0}{4} \left| \frac{\sin(\pi N \Phi_x / (N - 1) \Phi_0)}{\sin(\pi \Phi_x / (N - 1) \Phi_0)} \right|, \quad (17)$$

and exact zeros of the interference pattern appear at fractional values of the flux quantum, $\Phi_x = k(N - 1)\Phi_0/N$, with $k = 1, \dots, N - 1$. For large N we recover the typical expression of the Fraunhofer interference pattern, $I_c(\Phi_x) = \frac{\tau I_0 (N - 1)}{4} |\text{sinc}(\pi \Phi_x / \Phi_0)|$, with $\text{sinc}(x) = \sin(x)/x$ (the factor $1/4$ comes from the first order expansion in τ of Eq. (6)) [46], with zeros appearing at integer values of the flux quantum, $\Phi_x = k\Phi_0$.

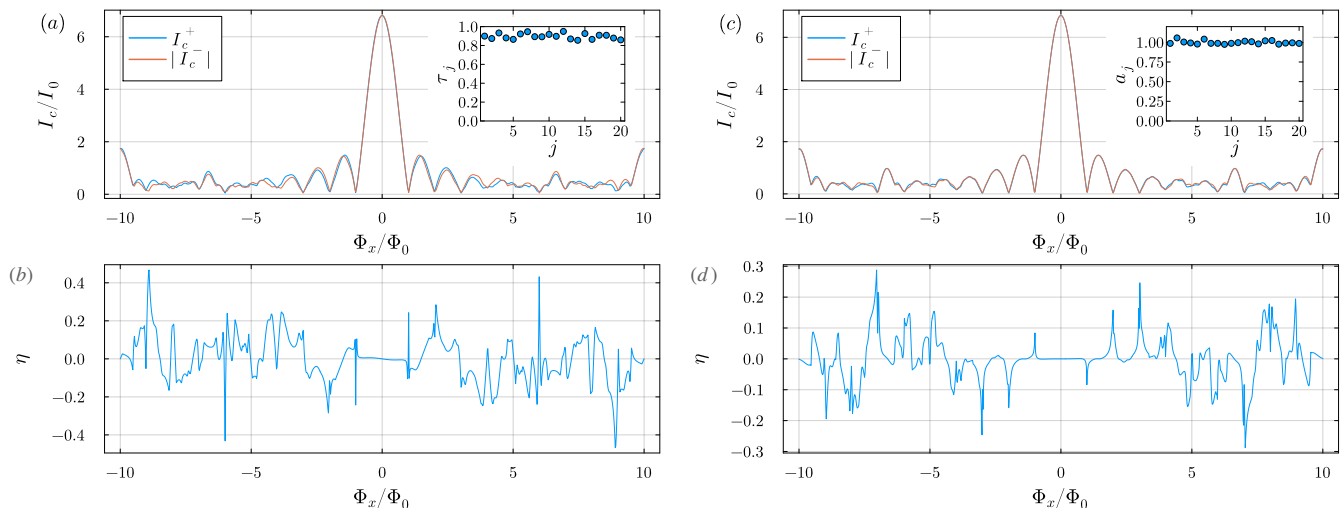


FIG. 3. Interference pattern of the critical currents $I_c^\pm(\Phi_x)$ of a multi-loop SQUID composed by $N = 20$ junctions as a function of the total flux Φ_x through the junction, as arising from the EPR Eq. (14). (a) Equal area junctions with random transparencies (shown in the inset). (b) Associated rectification coefficient. (c) Equal transmission $\tau = 0.9$ junctions with random areas (shown in the inset). (d) Associated rectification coefficient.

For general transparency τ , a closed expression for the critical current cannot be derived, and we have to resort to numerics. No exact zero appears in the Fraunhofer pattern; however, for fractional values of the flux $\Phi_x = k(N-1)\Phi_0/N$, the critical current generally displays minima. Indeed, the amplitudes of the current $A_n(k) = \sin(\pi nk)/\sin(\pi nk/N)$ are zero unless for kn multiple of N . For N even, the critical current has a secondary maximum at $k = N/2$ that involves only even n harmonics, so it is on the order of τ^2 . For N prime number, the current at the minima has only harmonics that are multiples of N , so that it is on order τ^N , and for general $N = pq$ the critical current at the minima is on order of $\tau^{\min(p,q)}$.

In the case of broken mirror symmetry, it is easily shown that for $\tau_j \ll 1$, such that only the first harmonic of the CPR is non-negligible, no diode effect arises. Indeed, by introducing $Z(\Phi_x) \equiv \sum_{j=1}^N \epsilon_{1,j} e^{i \sum_{k < j} \varphi_{x,k}(\Phi_x)}$, we can write

$$I(\varphi) = 2I_0 |Z(\Phi_x)| \sin(\varphi - \arg(Z(\Phi_x))), \quad (18)$$

from which by noticing that $|Z(\Phi_x)| = |Z(-\Phi_x)|$ immediately follows that $I_c^+(\Phi_x) = -I_c^-(\Phi_x)$.

To see the appearance of the diode effect, the transmissions τ_j need to be sizable, and we need to break the mirror symmetry of the system. This can be accomplished in two ways, *i*) by considering different transparencies τ_j and same areas of the loops, for which $\varphi_{x,j} = 2\pi(j-1)\Phi_x/N\Phi_0$, or *ii*) by keeping the same transparency τ for the junctions and considering different areas A_j of the loops, such that $\varphi_{x,j} = 2\pi \sum_{i \leq j} A_j B/\Phi_0$.

A. Equal areas and different junction transparencies

For the case in which the fluxes through the loops are all equal, $\varphi_{x,j} = 2\pi(j-1)\Phi_x/N\Phi_0 \equiv (j-1)\varphi_x$, but the junctions have different transparencies τ_j , by simple manipulations it can be shown that if the junctions are not inversion symmetric under the transformation $j \rightarrow N+1-j$, such that $\epsilon_{n,j} \neq \epsilon_{n,N+1-j}$, we have

$$I(\varphi, \Phi_x) \neq I(\varphi + 2\pi(N-1)\Phi_x/N\Phi_0, -\Phi_x), \quad (19)$$

so that we cannot rule out a diode effect.

An example of a Fraunhofer interference pattern for a parallel of junctions with the transmission randomly distributed between $0.85 < \tau_j < 0.95$ is shown in Fig. 3(a) (the inset shows the particular configuration of transmissions). A non-reciprocal Fraunhofer interference pattern appears with $I_c^+(\Phi_x) \neq |I_c^-(\Phi_x)|$, with a diode effect with a rectification up to a 40% percent, as shown in Fig. 3(b). However, high values of the rectification appear for fractional values of the flux quantum, for which either one of I_c^\pm becomes very small.

B. Equal transparencies and different loop areas

An analogous and alternative reciprocity symmetry breaking can be obtained by randomizing the fluxes $\varphi_{x,j}$. In Fig. 3(c), we show the critical currents I_c^\pm for the case in which $N = 20$ junctions have all transparency $\tau = 0.9$ and enclose each a slightly random flux, due to nonuniformity in the areas of the device. In particular, we assume that $A_j = A_{\text{tot}}(1 - \epsilon)/(N-1) + \delta A_j$, with $\sum_{j=1}^{N-1} \delta A_j = \epsilon A_{\text{tot}}$, in a way that we can study different

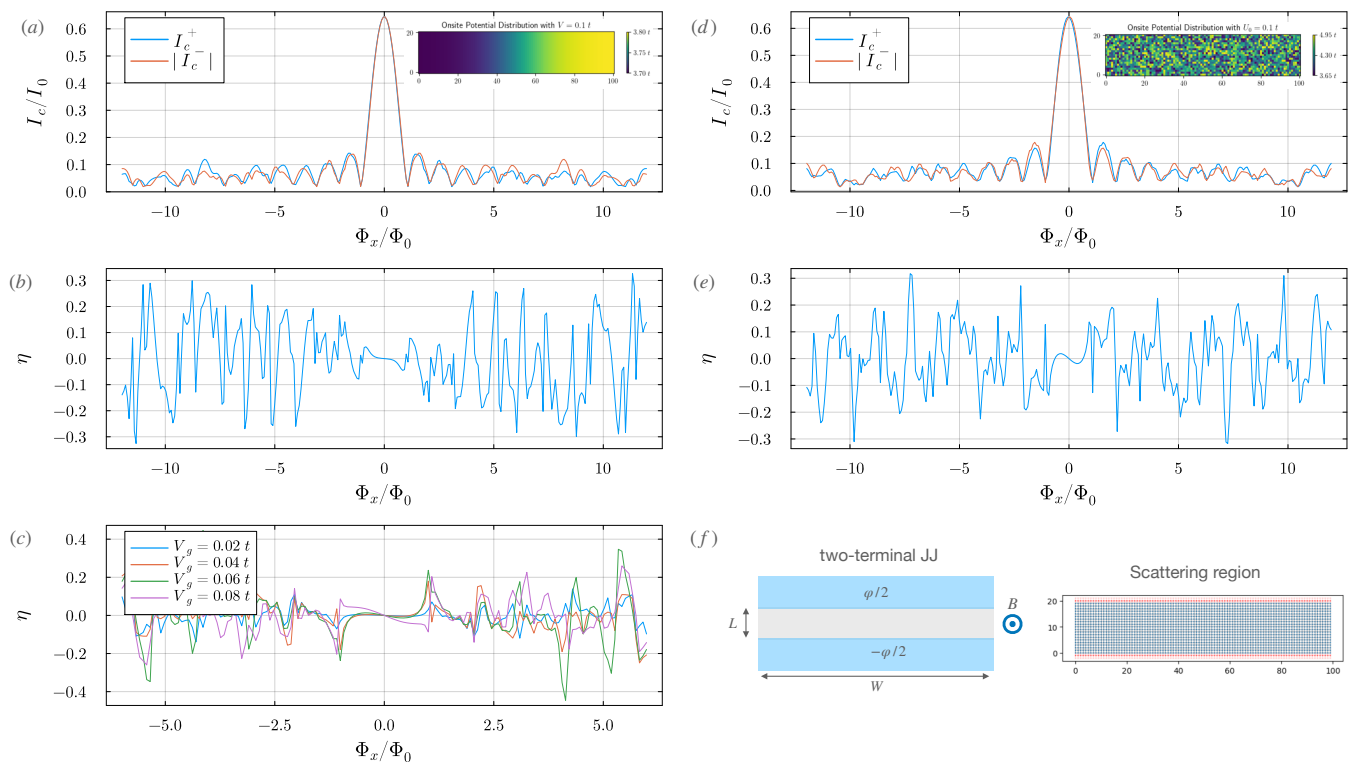


FIG. 4. Fraunhofer interference pattern for a planar wide Josephson junction schematically depicted in (f), in which two superconducting terminals kept at phase different φ are contacted to a normal region of width W , length L , and pierced by a magnetic field B that induces a flux $\Phi_x = BA$ through the normal region, with $A = WL$ the area of the central normal region. (a) Critical currents I_c^\pm as a function of the external flux Φ_x resulting from the local onsite potential $U_i = V(\tanh((x_i - W/2)/W_c) + 1)/2 + 4t - \mu$, for $V = 0.1 t$, $\mu = 0.3 t$, and $W_c = 20 a$, shown in the top-right inset. (b) Rectification coefficient η for the critical currents shown in (a). (c) Dependence of the rectification coefficient η of (b) on the gate potential $V = V_g$, for different values of V_g . (d) Critical currents I_c^\pm as a function of the external flux Φ_x resulting from the local onsite potential $U_i = \delta U_i + 4t - \mu$, with $-U_0/2 < \delta U_i < U_0/2$ randomly distributed for $U_0 = 0.1 t$ and $\mu = 0.3 t$, shown in the top-right inset. (e) Rectification coefficient η for the critical currents shown in (d). (f) Schematics of the wide Josephson junction and square lattice of lateral dimensions $W = 100 a$ and $L = 20 a$, in terms of a microscopic unit length a , employed in the tight-binding model to calculate the scattering matrix. Semi-infinite leads are attached to the scattering region's top and bottom. A potential barrier of strength $U_{\text{pot}} = 0.2 t$ is added at the interface with the leads.

disorder configurations with the same total area A_{tot} , and choose $\epsilon = 0.1$. The interference pattern is generally no longer a periodic flux function due to the area difference. In Fig. 3(d), we see that the rectification can reach up to 20% and, as in the case of random transparencies, the most significant rectification values are observed around integer flux quanta.

The full capability of the device to show rectification has been addressed in Ref. [18, 19], where devices composed of randomly chosen transparencies and/or randomly chosen areas have been optimized to obtain the highest values of rectification. Generally, a very disordered junction, composed of very low and very high transparency links, can give rise to strong rectification. However, the interference pattern deviates strongly from a Fraunhofer one since destructive interference is ineffective, and the critical current is always finite and sizable.

IV. WIDE JOSEPHSON JUNCTION

The analysis of the critical currents of a multi-loop parallel of highly transparent Josephson junctions discussed in Sec. III revealed a Fraunhofer pattern typical of wide Josephson junctions exposed to a magnetic field. The latter comprises an extended normal central region connected to two wide superconducting leads, schematically depicted in Fig. 4(f). Wide junctions comprise both three-dimensional systems enclosing a thick nonsuperconducting slab, with the external magnetic field in the plane of the junction [46], or two-dimensional systems with two (or multiple) superconducting leads. In this case, the magnetic field is perpendicular to the plane of the two-dimensional central region.

Here, we focus on two-terminal systems and extend the analysis of the diode effect to highly transparent, spatially inhomogeneous junctions. In particular, we consider two instances of spatial inhomogeneity: *i*) a geo-

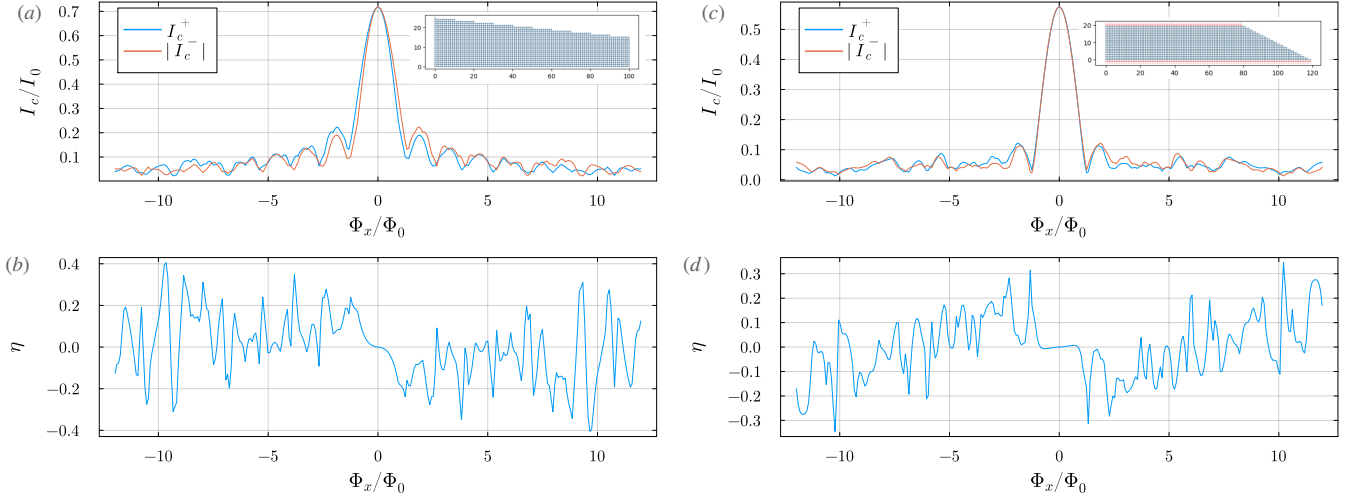


FIG. 5. (a) Critical currents I_c^\pm as a function of the external flux Φ_x for the trapezoidal junction shown in the top-right inset, with width $W = 100 a$ and left and right length $L_l = 25 a$, $L_r = 15 a$. (b) Rectification coefficient η for the critical currents shown in (a). (c) Critical currents I_c^\pm as a function of the external flux Φ_x for the trapezoidal junction shown in the top-right inset, with bottom and top width $W_b = 120 a$, $W_t = 80 a$, and length $L = 20 a$. (d) Rectification coefficient η for the critical currents shown in (c). For all panels we set $\mu = 0.3 t$, barrier $0.2 t$, and $\delta U_i = 0$.

metric inversion symmetric ballistic junction with a spatially varying potential in the central area, and *ii*) a clean ballistic system with a trapezoidal geometric shape, both breaking the spatial inversion symmetry of the system. As for the case *i*), we consider both long and short wavelength varying potentials as those generated by a side or back gate or by disorder, respectively.

We model the central region using a generic tight-binding model on a square lattice described by the Hamiltonian

$$H_c = \sum_{i,\sigma} U_i c_{i\sigma}^\dagger c_{i\sigma} - t \sum_{\langle i,j \rangle \sigma} e^{i\theta_{i,j}} c_{i\sigma}^\dagger c_{j\sigma} + \text{H.c.}, \quad (20)$$

where $c_{i\sigma}$ describe electrons with spin $\sigma = \uparrow, \downarrow$ at position \mathbf{r}_i , and the index i runs over all the lattice points of the central region. Electrons have onsite energy $U_i = 4t - \mu + \delta U_i$, comprising a chemical potential contribution μ and an additional onsite potential δU_i , and can hop among nearest neighboring sites with amplitude $-te^{i\theta_{i,j}}$, where the Peierls phase $\theta_{i,j} = \frac{e}{\hbar} \int_{\mathbf{r}_i}^{\mathbf{r}_j} \mathbf{A}(\mathbf{r}) \cdot d\mathbf{s}$ is due to the external magnetic field $\mathbf{B} = \nabla \times \mathbf{A}$. The central region is attached to the superconducting leads, and potential barriers shifting the local energy are added to the contact interface. We consider transport at zero energy in the large gap limit and numerically simulate several systems employing the KWANT package [47].

We first consider a central rectangular region of width $W = 100 a$ and length $L = 20 a$, in terms of a microscopic discretization length a , schematized in Fig. 4(f). We set the chemical potential to $\mu = 0.3 t$ both in the central region and in the leads, yielding approximately 20 open channels, and apply a non-uniform potential $\delta U_i = V(\tanh((x_i - W/2)/L_s) + 1)/2$. The potential is shown in the top-right inset of Fig. 4(a) for a value of

$V = 0.1 t$, yielding a smooth profile that changes on a length $L_s = 20 a$. In addition, potential barriers shifting the local energy by $0.2 t$ are added at the interface with the contacts. In Fig. 4(a), we show the associated Fraunhofer interference pattern for the critical currents I_c^\pm . We see that the presence of a smooth potential is sufficient to break the overall inversion symmetry of the junction and yields a diode effect, as quantified by the rectification coefficient η shown in Fig. 4(b), reaching up to 30% rectification.

The fact that a smooth, long wavelength potential can yield a diode effect suggests that the latter can be tuned by applying a gate. The potential shown in the inset of Fig. 4 (a) well approximates that one produced by two back gates occupying the left and right sides of the junction. In Fig. 4 (c), we plot the rectification efficiency for a few values of the gate potential, $V_g/t = 0.02, 0.04, 0.06, 0.08$. Contrary to the expectation, apart from the central lobe, we see no clear systematic evolution of the curves for increasing gate strength, pointing to the fact that the gate potential affects the interfering Andreev paths in a non-simple way.

We then consider a short wavelength scattering potential with δU_i randomly distributed between $-U_0/2 < \delta U_i < U_0/2$, as shown in the inset of Fig. 4 (d) for $U_0 = 0.1 t$. The resulting Fraunhofer interference pattern for the critical currents I_c^\pm is shown in Fig. 4(d), together with the rectification coefficient in Fig. 4(e). Analogously to the previous case, the spatial inversion symmetry broken by the potential is sufficient to give a diode effect in the Fraunhofer interference pattern that is qualitatively very similar to the case of a smooth uniform potential of Fig. 4(a,b).

In Fig. 5, we show the Fraunhofer interference pattern

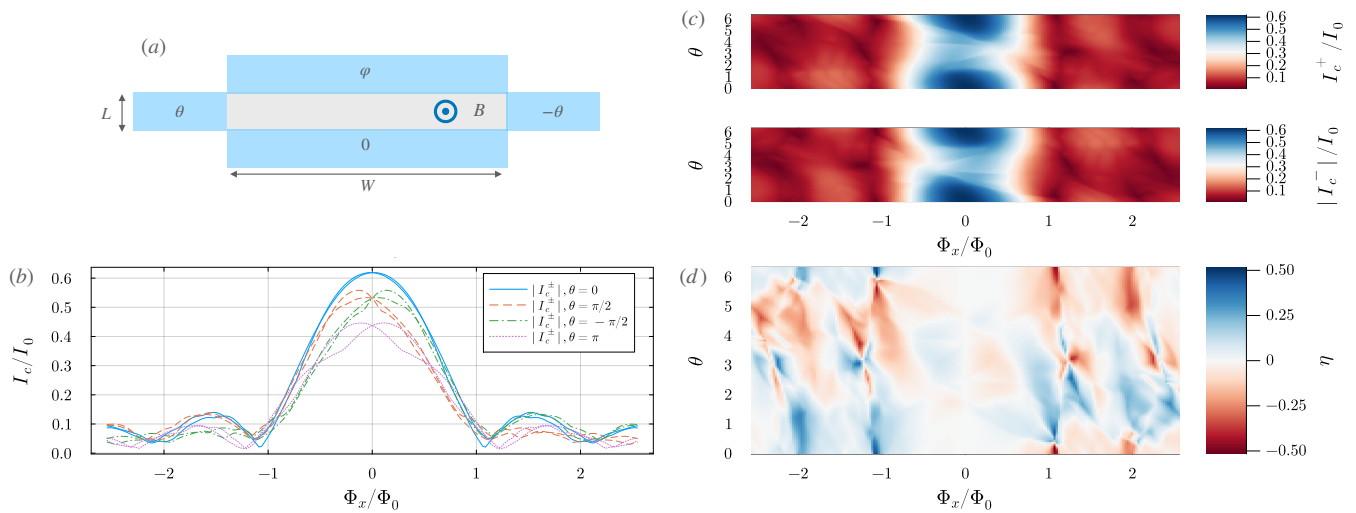


FIG. 6. (a) Schematics of a four-terminal planar Josephson junction, in which the bottom terminal serves as phase reference, and the top, left, and right terminals are kept at phase $\varphi, \theta, -\theta$, respectively. The central normal region has width W , length L , pierced by a magnetic field B that induces a flux $\Phi_x = BLW$. (b) Critical currents I_c^\pm as a function of the external flux Φ_x for four selected values of the phase $\theta = 0, \pm\pi/2, \pi$, with the entire (θ, Φ_x) -dependence shown in (c). (d) Rectification coefficient η for the critical currents shown in (c).

for the critical currents I_c^\pm for case *ii*) of a clean system with a trapezoidal shape. We consider two possible cases, one in which the distance between the two leads varies with the lateral position, shown in Fig. 5 (a), and one in which the size of the leads is different, shown in Fig. 5 (c). We see that the shape of the central region is sufficient to break the overall inversion symmetry of the junction, yielding a diode effect, as quantified by the rectification coefficient η shown Fig. 5 (b) and (d), reaching up to 40%. In Fig. 5(a), we see that the position-dependent distance between the leads for the entire structure yields a phase averaging that suppresses destructive interference. In contrast, in Fig. 5 (c), the phase averaging arises from additional trajectories on the system's right side. In the present case, the system is fully ballistic and coherent, and the averaging effect is solely due to the geometry that introduces paths with different lengths that add up to build the interference pattern.

V. MULTI-TERMINAL

The analysis presented for a two-terminal wide Josephson junction can be straightforwardly extended to the multi-terminal case. To observe a Fraunhofer pattern, we assume two wide contacts are attached to a wide central normal scattering region, plus additional lateral superconducting leads. In particular, to study the onset of a diode effect in the Fraunhofer pattern, we consider a four-terminal symmetric structure, with a bottom wide contact kept at phase zero for reference, a top contact kept at phase φ with respect to the bottom terminal, and the lateral terminals kept at phase difference $\pm\theta$ with respect

to the reference terminal. The system is schematized in Fig. 6(a).

As explained in Sec. II B, in a mirror-symmetric setup, with $\varphi_L = \theta$ and $\varphi_R = -\varphi_L$, the critical currents between the top and bottom terminals satisfy

$$I_c^+(\theta, -\theta, \Phi_x) = -I_c^-(\theta, \theta, \Phi_x), \quad (21)$$

where the mirror symmetry maps $\theta \rightarrow -\theta$. This is seen in Fig. 6 (b), where we show the critical currents for four selected phase difference values $\theta = 0, \pm\pi/2, \pi$. For $\theta = 0$, we expect no difference in the I_c^\pm , and the observed slight difference is ascribed to imperfection in the system modelization. For $\theta = \pi$ we see that $I_c^+(\pi, -\pi, \Phi_x) = -I_c^-(\pi, \pi, -\Phi_x)$ and more generally we observe the behavior dictated by Eq. 21, as can be checked also in the entire (θ, Φ_x) dependence of I_c^\pm shown in Fig. 6 (c) and in the rectification coefficients shown in Fig. 6(d).

This setup shows how the magnetic flux through the central region can control the diode effect in a mirror-symmetric system.

VI. SUMMARY AND CONCLUSIONS

In this work, we studied the Fraunhofer interference pattern in two-terminal and four-terminal Josephson junctions, focusing on the role of spatial inhomogeneity in inducing the diode effect. As a first step, we address the general conditions that allow for the appearance of a diode when the mirror symmetry of the junction, with respect to a plane defined by the cross product between the direction of the applied external orbital magnetic field

and the bias current (see Fig. 1), is broken, both in two-terminal and multi-terminal systems.

We then studied a multi-loop circuit of highly transparent Josephson junctions connected in parallel. In such a system, a Fraunhofer interference pattern arises for disorder in the transparency of the junctions or in the fluxes through the areas of the multi-loop structure. The latter originate from slightly different areas in a typical experimental configuration. Interestingly, we notice that the disorder in the fluxes can have different origins apart from random areas in an extended junction, that can occur due to finite kinetic inductance in the system [32]. The multi-loop parallel circuit of highly transparent junctions has been shown to yield a sizable diode effect for random configurations, and it has been optimized for high rectification in Refs. [18, 19]. In the devices showing maximal efficiency, the destructive interference induced by the magnetic field results to be spoiled, with the associated interference pattern found to be highly deviating from a Fraunhofer one.

Subsequently, we studied planar two-terminal junctions that include a normal region, and we induce spatial mirror symmetry breaking in two ways: by introducing a local potential in the normal region that may arise either due to a long wavelength modulation or by short wavelength disorder. The case of long wavelength modulation well describes the effect of bottom and side gates that tune the local charge density and induce a spatial modulation of the transparency. However, apart from the central lobe of the Fraunhofer pattern, the rectification coefficient shows no clear dependence on the gate potential. In general, we see a qualitative correspondence between the Fraunhofer pattern of a wide junction and the one of a multi-loop parallel of Josephson junctions that is not a priori obvious since there is no generalization of the EPR Eq. 6 in terms of transmission coefficients in presence of orbital magnetic field. Nevertheless, the analogy also holds microscopically for negligible interchannel coupling in the central area and negligible non-local Andreev reflection.

Finally, we extend the result to a four-terminal device, showing how a phase difference on the control leads yields rectification for finite external magnetic fields, providing an additional knob for tuning the diode effect.

The analysis presented sheds light on the ubiquity of the diode effect in Josephson junctions, showing how spatial-inversion symmetry breaking originating from different kind of disorder realizations produce qualitatively similar diode effect in the Fraunhofer diffraction pattern of multi-terminal systems.

VII. ACKNOWLEDGMENTS

We acknowledge S. Heun for valuable discussions and for carefully reading the manuscript. M.C. and F.G. acknowledge the EU's Horizon 2020 Research and Innovation Framework Programme under Grants No.

964398 (SUPERGATE) and the PNRR MUR project PE0000023-NQSTI for partial financial support. F.G. acknowledges partial financial support under Grant No. 101057977 (SPECTRUM). E.S. acknowledges the project HelicS, project number DFM.AD002.206. We acknowledge NextGenerationEU PRIN project 2022A8CJP3 (GAMESQUAD) for partial financial support.

Appendix A: Scattering matrix approach

Here, we briefly review the derivation of the Andreev spectrum of a wide junction, and we extend it to the case of multi-terminal Josephson junctions in the short junction approximation [41].

We consider a generic normal scattering region connected to M superconducting terminals that, for simplicity, we assume to have the same equal superconducting gap Δ . Each terminal has n_i open channels, and transport along these channels and through the central region is described by a unitary scattering matrix s that has a block structure, with the block $s_{i,j}$ of dimensions $n_i \times n_j$. Unitarity $s^\dagger s = 1$ ensures overall current conservation. The Andreev spectrum is obtained by solving the eigenproblem [40, 43]

$$s_A s_N \psi = \psi, \quad (\text{A1})$$

where the normal (N) and Andreev (A) scattering matrices are given by

$$s_N = \begin{pmatrix} s(\epsilon) & 0 \\ 0 & s^*(-\epsilon) \end{pmatrix}, \quad s_A = \alpha \begin{pmatrix} 0 & r_A^* \\ r_A & 0 \end{pmatrix}, \quad (\text{A2})$$

with $r_A = \text{diag}(e^{i\varphi_1}, \dots, e^{i\varphi_M})$, and $\alpha = \exp(-i \arccos(\epsilon/\Delta))$. In the Andreev approximation of a scattering region of linear size much smaller than the coherence length $\xi = \hbar v_F/\Delta$, we can neglect the energy dependence of the scattering matrix s , so that $s(\epsilon) = s(-\epsilon) \equiv s$. Following Ref. [41], the Andreev spectrum is therefore determined by

$$\begin{pmatrix} 0 & s^\dagger r_A^* \\ s^T r_A & 0 \end{pmatrix} \psi = \alpha \psi. \quad (\text{A3})$$

We can transform the eigenvalue problem $X\psi = \alpha\psi$ in a way that $\frac{1}{2}(X+X^{-1})\psi = \frac{1}{2}(\alpha+\alpha^{-1})\psi = \frac{\epsilon}{\Delta}\psi$, so that the general Andreev spectrum is obtained as an eigenvalue problem can be cast in the form of Eq. (4).

Appendix B: High harmonic Josephson elements

The EPR of Eq. (6) describes a general Andreev bound state between two superconducting leads and across a high transparency normal region. It has a general functional form on the phase difference and can also arise in the case of a series of two Josephson junctions, as shown in Ref. [19].

For the case of an Andreev state, the current can also be calculated as a series expansion in the tunnel transparency by considering multiple Cooper pair transport across the junction through standard techniques of many-body theory [48]. One of the characteristics of the EPR Eq. (6) is the alternation in sign between the even and odd harmonics, which is rooted in the Andreev reflection phase " i " at zero energy. This way, a net Cooper pair is transferred between two superconducting leads through a barrier of transmission τ through two Andreev reflections at the two superconducting leads, thus carrying a π phase-shift.

A direct calculation of the Fourier component of the Andreev state EPR confirms the sign alternation of even and odd harmonics and reads [49]

$$E(\varphi)/\Delta = -\epsilon_0 - 2 \sum_{n=1}^{\infty} \epsilon_n \cos(n\varphi), \quad (\text{B1})$$

with the coefficients ϵ_n given by

$$\epsilon_n = \frac{\tau^n}{4^n} \frac{\Gamma(3/2)}{n! \Gamma(3/2 - n)} {}_2F_1(n - 1/2, n + 1/2; 1 + 2n, \tau), \quad (\text{B2})$$

where $\Gamma(z)$ is the Gamma function and ${}_2F_1(a, b; c; z)$ is the hypergeometric function [50]. The coefficients $\epsilon_n = (-1)^{n+1} |\epsilon_n|$ are positive for odd n and negative for even n .

-
- [1] R. Upadhyay, D. S. Golubev, Y.-C. Chang, G. Thomas, A. Guthrie, J. T. Peltonen, and J. P. Pekola, Microwave quantum diode, *Nature Communications* **15**, 630 (2024).
- [2] F. Ando, Y. Miyasaka, T. Li, J. Ishizuka, T. Arakawa, Y. Shiota, T. Moriyama, Y. Yanase, and T. Ono, Observation of superconducting diode effect, *Nature* **584**, 373 (2020).
- [3] C. Baumgartner, L. Fuchs, A. Costa, S. Reinhardt, S. Gronin, G. C. Gardner, T. Lindemann, M. J. Manfra, P. E. Faria Junior, D. Kochan, J. Fabian, N. Paradiso, and C. Strunk, Supercurrent rectification and magnetochiral effects in symmetric josephson junctions, *Nature Nanotechnology* **17**, 39 (2022).
- [4] L. Bauriedl, C. Bäuml, L. Fuchs, C. Baumgartner, N. Paulik, J. M. Bauer, K.-Q. Lin, J. M. Lupton, T. Taniguchi, K. Watanabe, C. Strunk, and N. Paradiso, Supercurrent diode effect and magnetochiral anisotropy in few-layer nbse2, *Nature Communications* **13**, 4266 (2022).
- [5] E. Strambini, M. Spies, N. Ligato, S. Ilić, M. Rouco, C. González-Orellana, M. Ilyn, C. Rogero, F. S. Bergeret, J. S. Moodera, P. Virtanen, T. T. Heikkilä, and F. Gazotto, Superconducting spintronic tunnel diode, *Nature Communications* **13**, 2431 (2022).
- [6] A. Costa, C. Baumgartner, S. Reinhardt, J. Berger, S. Gronin, G. C. Gardner, T. Lindemann, M. J. Manfra, J. Fabian, D. Kochan, N. Paradiso, and C. Strunk, Sign reversal of the josephson inductance magnetochiral anisotropy and $0 - \pi$ -like transitions in supercurrent diodes, *Nature Nanotechnology* **18**, 1266 (2023).
- [7] M. Nadeem, M. S. Fuhrer, and X. Wang, The superconducting diode effect, *Nature Reviews Physics* **5**, 558 (2023).
- [8] R. Wakatsuki, Y. Saito, S. Hoshino, Y. M. Itahashi, T. Ideue, M. Ezawa, Y. Iwasa, and N. Nagaosa, Nonreciprocal charge transport in noncentrosymmetric superconductors, *Science Advances* **3**, e1602390 (2017), <https://www.science.org/doi/pdf/10.1126/sciadv.1602390>.
- [9] E. Zhang, X. Xu, Y.-C. Zou, L. Ai, X. Dong, C. Huang, P. Leng, S. Liu, Y. Zhang, Z. Jia, X. Peng, M. Zhao, Y. Yang, Z. Li, H. Guo, S. J. Haigh, N. Nagaosa, J. Shen, and F. Xiu, Nonreciprocal superconducting nbse2 antenna, *Nature Communications* **11**, 5634 (2020).
- [10] Y. M. Itahashi, T. Ideue, Y. Saito, S. Shimizu, T. Ouchi, T. Nojima, and Y. Iwasa, Nonreciprocal transport in gate-induced polar superconductor $\text{SrTiO}_3/\text{LaAlO}_3$, *Science Advances* **6**, eaay9120 (2020), <https://www.science.org/doi/pdf/10.1126/sciadv.aay9120>.
- [11] Y.-Y. Lyu, J. Jiang, Y.-L. Wang, Z.-L. Xiao, S. Dong, Q.-H. Chen, M. V. Milošević, H. Wang, R. Divan, J. E. Pearson, P. Wu, F. M. Peeters, and W.-K. Kwok, Superconducting diode effect via conformal-mapped nanoholes, *Nature Communications* **12**, 2703 (2021).
- [12] H. Narita, J. Ishizuka, R. Kawarazaki, D. Kan, Y. Shiota, T. Moriyama, Y. Shimakawa, A. V. Ognev, A. S. Samardak, Y. Yanase, and T. Ono, Field-free superconducting diode effect in noncentrosymmetric superconductor/ferromagnet multilayers, *Nature Nanotechnology* **17**, 823 (2022).
- [13] J.-X. Lin, P. Siriviboon, H. D. Scammell, S. Liu, D. Rhodes, K. Watanabe, T. Taniguchi, J. Hone, M. S. Scheurer, and J. I. A. Li, Zero-field superconducting diode effect in small-twist-angle trilayer graphene, *Nature Physics* **18**, 1221 (2022).
- [14] N. F. Q. Yuan and L. Fu, Supercurrent diode effect and finite-momentum superconductors, *Proceedings of the National Academy of Sciences* **119**, e2119548119 (2022), <https://www.pnas.org/doi/pdf/10.1073/pnas.2119548119>.
- [15] B. Pal, A. Chakraborty, P. K. Sivakumar, M. Davydova, A. K. Gopi, A. K. Pandeya, J. A. Krieger, Y. Zhang, M. Date, S. Ju, N. Yuan, N. B. M. Schröter, L. Fu, and S. S. P. Parkin, Josephson diode effect from cooper pair momentum in a topological semimetal, *Nature Physics* **18**, 1228 (2022).
- [16] S. Y. F. Zhao, X. Cui, P. A. Volkov, H. Yoo, S. Lee, J. A. Gardener, A. J. Akey, R. Engelke, Y. Ronen, R. Zhong, G. Gu, S. Plugge, T. Tummuru, M. Kim, M. Franz, J. H. Pixley, N. Poccia, and P. Kim, Time-reversal symmetry breaking superconductivity between twisted cuprate superconductors, *Science* **382**, 1422 (2023),

- <https://www.science.org/doi/pdf/10.1126/science.abl8371>.
- [17] S. Ghosh, V. Patil, A. Basu, Kuldeep, A. Dutta, D. A. Jangade, R. Kulkarni, A. Thamizhavel, J. F. Steiner, F. von Oppen, and M. M. Deshmukh, High-temperature josephson diode, *Nature Materials* **23**, 612 (2024).
 - [18] R. S. Souto, M. Leijnse, and C. Schrade, Josephson diode effect in supercurrent interferometers, *Phys. Rev. Lett.* **129**, 267702 (2022).
 - [19] A. M. Bozkurt, J. Brookman, V. Fatemi, and A. R. Akhmerov, Double-Fourier engineering of Josephson energy-phase relationships applied to diodes, *SciPost Phys.* **15**, 204 (2023).
 - [20] D. Margineda, A. Crippa, E. Strambini, Y. Fukaya, M. T. Mercaldo, M. Cuoco, and F. Giazotto, Sign reversal diode effect in superconducting dayem nanobridges, *Communications Physics* **6**, 343 (2023).
 - [21] A. Greco, Q. Pichard, and F. Giazotto, Josephson diode effect in monolithic dc-SQUIDS based on 3D Dayem nanobridges, *Applied Physics Letters* **123**, 092601 (2023), <https://pubs.aip.org/aip/apl/article-pdf/doi/10.1063/5.0165259/18279784/092601.1.5.0165259.pdf>.
 - [22] A. Greco, Q. Pichard, E. Strambini, and F. Giazotto, Double loop dc-SQUID as a tunable Josephson diode, *Applied Physics Letters* **125**, 072601 (2024), <https://pubs.aip.org/aip/apl/article-pdf/doi/10.1063/5.0211021/20112024/072601.1.5.0211021.pdf>.
 - [23] M. Gupta, G. V. Graziano, M. Pendharkar, J. T. Dong, C. P. Dempsey, C. Palmstrøm, and V. S. Pribiag, Gate-tunable superconducting diode effect in a three-terminal josephson device, *Nature Communications* **14**, 3078 (2023).
 - [24] F. Zhang, A. S. Rashid, M. Tanhayi Ahari, G. J. de Coster, T. Taniguchi, K. Watanabe, M. J. Gilbert, N. Samarth, and M. Kayyalha, Magnetic-field-free non-reciprocal transport in graphene multiterminal josephson junctions, *Phys. Rev. Appl.* **21**, 034011 (2024).
 - [25] C. Ciaccia, R. Haller, A. C. C. Drachmann, T. Lindemann, M. J. Manfra, C. Schrade, and C. Schönenberger, Gate-tunable josephson diode in proximitized inas supercurrent interferometers, *Phys. Rev. Res.* **5**, 033131 (2023).
 - [26] D. Margineda, A. Crippa, E. Strambini, Y. Fukaya, M. T. Mercaldo, C. Ortix, M. Cuoco, and F. Giazotto, Back-action supercurrent diodes, *arXiv e-prints*, arXiv:2311.14503 (2023), arXiv:2311.14503 [cond-mat.mes-hall].
 - [27] G. De Simoni and F. Giazotto, Quasi-ideal feedback-loop supercurrent diode, *Physical Review Applied* **21**, 064058 (2024).
 - [28] Y. Hou, F. Nichele, H. Chi, A. Lodesani, Y. Wu, M. F. Ritter, D. Z. Haxell, M. Davydova, S. Ilić, O. Glezakou-Elbert, A. Varambally, F. S. Bergeret, A. Kamra, L. Fu, P. A. Lee, and J. S. Moodera, Ubiquitous superconducting diode effect in superconductor thin films, *Phys. Rev. Lett.* **131**, 027001 (2023).
 - [29] A. Sundaresh, J. I. Väyrynen, Y. Lyanda-Geller, and L. P. Rokhinson, Diamagnetic mechanism of critical current non-reciprocity in multilayered superconductors, *Nature Communications* **14**, 1628 (2023).
 - [30] V. M. Krasnov, V. A. Oboznov, and N. F. Pedersen, Fluxon dynamics in long josephson junctions in the presence of a temperature gradient or spatial nonuniformity, *Phys. Rev. B* **55**, 14486 (1997).
 - [31] T. Golod and V. M. Krasnov, Demonstration of a superconducting diode-with-memory, operational at zero magnetic field with switchable nonreciprocity, *Nature Communications* **13**, 3658 (2022).
 - [32] S. Chen, S. Park, U. Vool, N. Maksimovic, D. A. Broadway, M. Flaks, T. X. Zhou, P. Maletinsky, A. Stern, B. I. Halperin, and A. Yacoby, Current induced hidden states in josephson junctions, *Nature Communications* **15**, 8059 (2024).
 - [33] J. J. He, Y. Tanaka, and N. Nagaosa, A phenomenological theory of superconductor diodes, *New Journal of Physics* **24**, 053014 (2022).
 - [34] A. Daido and Y. Yanase, Superconducting diode effect and nonreciprocal transition lines, *Phys. Rev. B* **106**, 205206 (2022).
 - [35] S. Ilić and F. S. Bergeret, Theory of the supercurrent diode effect in rashba superconductors with arbitrary disorder, *Phys. Rev. Lett.* **128**, 177001 (2022).
 - [36] Y. Yerin, S.-L. Drechsler, A. A. Varlamov, M. Cuoco, and F. Giazotto, Supercurrent rectification with time-reversal symmetry broken multiband superconductors, *Phys. Rev. B* **110**, 054501 (2024), arXiv:2404.12641 [cond-mat.supr-con].
 - [37] Y. Fukaya, M. T. Mercaldo, D. Margineda, A. Crippa, E. Strambini, F. Giazotto, C. Ortix, and M. Cuoco, Design of supercurrent diode by vortex phase texture, *arXiv e-prints*, arXiv:2403.04421 (2024), arXiv:2403.04421 [cond-mat.supr-con].
 - [38] M. Roig, P. Kotetes, and B. M. Andersen, Superconducting diodes from magnetization gradients, *Phys. Rev. B* **109**, 144503 (2024).
 - [39] C. W. J. Beenakker, Universal limit of critical-current fluctuations in mesoscopic josephson junctions, *Phys. Rev. Lett.* **67**, 3836 (1991).
 - [40] C. W. J. Beenakker, Three “universal” mesoscopic josephson effects, in *Transport Phenomena in Mesoscopic Systems*, edited by H. Fukuyama and T. Ando (Springer Berlin Heidelberg, Berlin, Heidelberg, 1992) pp. 235–253.
 - [41] B. van Heck, S. Mi, and A. R. Akhmerov, Single fermion manipulation via superconducting phase differences in multiterminal josephson junctions, *Phys. Rev. B* **90**, 155450 (2014).
 - [42] J. Bardeen, R. Kümmel, A. E. Jacobs, and L. Tewordt, Structure of vortex lines in pure superconductors, *Phys. Rev.* **187**, 556 (1969).
 - [43] C. W. J. Beenakker, Random-matrix theory of quantum transport, *Rev. Mod. Phys.* **69**, 731 (1997).
 - [44] M. Coraiola, A. E. Svetogorov, D. Z. Haxell, D. Sabonis, M. Hinderling, S. C. ten Kate, E. Cheah, F. Krizek, R. Schott, W. Wegscheider, J. C. Cuevas, W. Belzig, and F. Nichele, Flux-tunable josephson diode effect in a hybrid four-terminal josephson junction, *ACS Nano* **18**, 9221 (2024).
 - [45] R. D. Luca, Quantum interference in josephson junctions, *Journal of Modern Physics* **6**, 526 (2015).
 - [46] M. Tinkham, *Introduction to Superconductivity*, 2nd ed. (Dover Publications, 2004).
 - [47] C. W. Groth, M. Wimmer, A. R. Akhmerov, and X. Waintal, Kwant: a software package for quantum transport, *New Journal of Physics* **16**, 063065 (2014).
 - [48] G. D. Mahan, *Many Particle Physics, Third Edition* (Plenum, New York, 2000).
 - [49] D. Willsch, D. Rieger, P. Winkel, M. Willsch, C. Dickel, J. Krause, Y. Ando, R. Lescanne, Z. Leghtas, N. T.

Bronn, P. Deb, O. Lanes, Z. K. Mineev, B. Dennig, S. Geisert, S. Günzler, S. Ihssen, P. Paluch, T. Reisinger, R. Hanna, J. H. Bae, P. Schüffelgen, D. Grützmacher, L. Buimaga-Iarinca, C. Morari, W. Wernsdorfer, D. P. DiVincenzo, K. Michielsen, G. Catelani, and I. M. Pop, Observation of josephson harmonics in tunnel junctions,

Nature Physics **20**, 815 (2024).
[50] I. S. Gradshteyn and I. M. Ryzhik, Table of Integrals, Series, and Products, seventh ed., edited by D. Zwillinger and V. H. Moll (Academic Press, 2007).